

Non-resonant dot-cavity coupling and its applications in resonant quantum dot spectroscopy

S. Ates^{(1)*}, S. M. Ulrich^{(1)*}, A. Ulhaq⁽¹⁾, S. Reitzenstein⁽²⁾,
A. Löffler⁽²⁾, S. Höfling⁽²⁾, A. Forchel⁽²⁾, & P. Michler⁽¹⁾

⁽¹⁾ *Institut für Halbleiteroptik und Funktionelle Grenzflächen,
Universität Stuttgart, Allmandring 3, 70569 Stuttgart, Germany, and*

⁽²⁾ *Technische Physik,
Universität Würzburg, Am Hubland,
97074 Würzburg, Germany.*

* *Email correspondence: s.ates@ihfg.uni-stuttgart.de; s.ulrich@ihfg.uni-stuttgart.de*

Promising solid-state single-photon sources and cavity quantum electrodynamic schemes have been realized on the basis of coupled quantum dot and micro-/nanocavity systems [1, 2]. Recent experimental studies on the single quantum dot (QD) level showed a pronounced emission at the cavity resonance even for strongly detuned dot-cavity systems [3, 4, 5]. This behaviour is indicative of a complex light-matter interaction in a semiconductor well beyond the widely used two-level emitter-cavity schemes. Different mechanisms such as photon-induced 'shake-up' processes in charged quantum dots [6], dephasing processes [7, 8, 9] and phonon-mediated processes [10] are currently discussed to understand the experimentally observed features. A well prepared and clearly defined experimental situation is therefore mandatory to gain a thorough understanding of the responsible physical mechanisms behind the non-resonant dot-cavity coupling.

Here we present experimental investigations on the non-resonant dot-cavity coupling of a single quantum dot inside a micro-pillar where the dot has been resonantly excited in the s-shell, thereby avoiding the generation of additional charges in the QD and its surrounding. As a direct proof of the pure single dot-cavity system, strong photon anti-bunching is consistently observed in the autocorrelation functions of the QD and the mode emission, as well as in the cross-correlation function between the dot and mode signals. Strong Stokes and anti-Stokes-like emission is observed for energetic QD-mode detunings of up to ~ 100 times the QD linewidth. Furthermore, we demonstrate that non-resonant dot-cavity coupling can be utilized to directly monitor and study relevant QD s-shell properties like fine-structure splittings, emission saturation and power broadening, as well as photon statistics with negligible background contributions.

Our results open a new perspective on the understanding and implementation of dot-cavity systems for single-photon sources, single and multiple quantum dot lasers, semiconductor cavity quantum electrodynamics, and their implementation, e.g. in quantum information technology [11].

High Q -factor nano- and micro-cavities can enhance or suppress the spontaneous emission of photons, e.g. from a quantum dot, coupled to a well defined mode by the Purcell effect

[12]. For very high- Q (i.e. weakly damped) cavities the spontaneous emission can even become a reversible process so that quantum entanglement of radiation and matter becomes possible, in the so-called *strong coupling* regime [12]. Resonantly coupled single quantum dot nano- and micro-cavity systems, i.e. with QD and cavity mode in resonance, have been realized both in the *weak coupling* [1, 13] and the *strong coupling* regime [14, 15, 16]. Recent experimental results also show significant emission at the cavity resonance even if the single quantum dot is not in resonance with the cavity mode [3, 4, 5]. Similar observations have also been reported from nano-cavity laser structures with only few QDs as the active medium [17]. This so-called *non-resonantly coupled emission* mechanism is not well understood and controversially discussed in the literature: Kaniber et al. [6] suggested that the experimentally observed coupling between a single QD and a photonic crystal cavity mode is mediated by photon-induced 'shake-up'-like processes in charged quantum dots. In their theoretical work [7, 9], Naesby et al. and Auffèves et al. demonstrated that *dephasing* shifts the emission intensity towards the cavity frequency, whereas Tarel and Savona [10] showed the important role of the *electron-acoustic-phonon interaction* for understanding the emission properties. From the experimental point of view it is desirable to study the coupling mechanism via purely resonant excitation of the QD s-shell in order to obtain a better understanding of the underlying physics. However, in all *experimental* studies such a *purely resonant excitation* of the QD s-shell has not been performed so far. The non-resonantly coupled system we use is based on individual self-assembled (In,Ga)As/GaAs QDs embedded in a high-quality micro-pillar cavity. To ensure single exciton generation and to suppress background emission we use *purely resonant s-shell excitation* of an uncharged QD at low temperatures ($T < 30$ K). Signatures of strong emission coupling are observed for both negative and positive spectral detunings between a single QD and the fundamental cavity mode. Furthermore, we demonstrate that the cavity mode emission can be conveniently used to monitor essential QD s-shell properties in high detail while avoiding the complications involved with direct investigations of the resonance fluorescence and/or transmission (e.g. stray light) and reflection experiments (e.g. nano-apertures, noisy background, or demand on high setup sensitivity).

For all investigations in the current work, a special orthogonal geometry of sample excitation and emission detection was used (**Fig. 1b**; for details, see methods section) in order to optically address and study the emission characteristics of single QDs in selected micro-pillar

structures. **Figure 1a** shows a characteristic low-temperature ($T = 22$ K) photoluminescence spectrum of a micro-pillar cavity under p-shell excitation of a single QD. Two emission lines are visible and are identified as excitonic emission from the QD (~ 1.3574 eV) and fundamental mode emission (~ 1.3577 eV) of the pillar cavity. In order to study the physical origin of the mode emission in more detail, photon auto- and cross-correlation measurements between the two lines have been performed and are displayed in **Figs. 1c - e**. All correlation measurements display pronounced photon anti-bunching. The *auto-correlation* of the single QD (trace **c**) displays perfect anti-bunching (i.e. $g^{(2)}(\tau = 0) = 0.0(2)$; deconvoluted value) as expected for a single quantum emitter [18]. Surprisingly, also the mode itself exhibits a strongly reduced $g^{(2)}(0)$ value of 0.20 ± 0.02 , demonstrating that the observed mode emission is mainly ($\sim 90\%$) originating from a single quantum emitter. The signature of strong photon anti-bunching even in the *cross-correlation* of these two lines (with $g^{(2)}(0) = 0.10 \pm 0.02$) demonstrates a pronounced *non-resonant dot-cavity coupling* between the same single QD and the ~ 280 μeV detuned pillar mode as was also consistently observed by other groups [3, 4] under non-resonant barrier pumping and p-shell excitation, respectively. The effect is not yet clarified from a theoretical perspective, thus making further detailed studies indispensable to gain a deeper understanding of the underlying processes. Furthermore, as we show in the following, this non-resonant dot-cavity coupling can be utilized to effectively transfer and 'monitor' the information of various relevant QD s-shell characteristics onto a nearly background-free coupled mode channel.

In **Figs. 2a** and **b**, the effect of non-resonant QD-cavity coupling is demonstrated for both *positive* and *negative* QD-mode detunings $\Delta E = +200$ μeV (-380 μeV) at $T = 10$ K (29 K). Excitation laser frequency scans are performed on the s-shell resonance of a single quantum dot, and the resulting spectra are displayed as a function of the laser-exciton detuning δ . Under consecutive variation of the laser frequency, two prominent effects can be clearly observed. First, a strong increase in the composite signal of the QD s-shell emission and scattered laser light demonstrates the excitation of *resonance fluorescence* from the quantum emitter. Furthermore, in parallel with the generation of resonance fluorescence, significant emission signal is also observed from the detuned pillar mode. Worth to note, this effect is found over a wide temperature range, with positive and negative QD-mode detunings of up to $\sim 100 \times$ the single quantum dot s-shell emission FWHM (or up to $\sim 4 \times$ the fundamental mode linewidth). In **Fig. 2c** we plot the *relative* mode emission intensity ratio, normalized

to the sum of QD and mode emission, as a function of QD-mode detuning ΔE . Each data point represents the conditions of fully resonant excitation ($\delta = 0$) into the QD s-shell at a constant power level ($P_0 = 300$ nW). Interestingly, a pronounced increase of the normalized mode intensity is traced with increasing temperature – in spite of the increasing QD-mode detuning $\Delta E(T)$. A large relative coupling efficiency of $\sim 72\%$ is observed from the collected signal. These results strongly support the recent suggestion that *phonon-mediated processes* may play a dominant role for the non-resonant dot cavity coupling [7, 10]. In particular, due to the resonant excitation process of single neutral excitons in the QD we can exclude photon-induced ‘shake-up’ processes [6] in our samples.

Figures 3a - d display results of laser resonance scan series (**a, b**: $T = 18$ K, **d**: $T = 26$ K) on the s-shell of the single QD in pillar 2, in direct comparison with the emission characteristics of the non-resonantly coupled pillar mode. In the corresponding top and bottom traces, each data point represents the integrated intensity derived from Lorentzian line fits to the mode (plots **a, c**) and the QD s-shell emission (plots **b, d**), respectively. As a consequence of resonant excitation the direct QD s-shell signal is composed of resonance fluorescence and laser stray light, reflected as a small non-vanishing background level for large detunings δ from the resonance (traces **b, d**). The data sets in **a** and **b** observed at $T = 18$ K reveal distinct doublet structures with similar linewidths and energy splittings ($\Delta E_{FSS} = 11 \pm 0.3 \mu\text{eV}$). The doublet structure of the excitonic line is caused by the electron-hole exchange interaction in an asymmetric QD [19]. In **Figs. 3c** and **d** the known effect of power broadening [20] of the excitonic line under resonant excitation is compared with the coupled mode emission. A significant line broadening is clearly visible under stepwise increasing laser powers, revealing high quantitative accordance between the FWHM of the μ -PL lines in the data sets **c** and **d**. Please note that these power-dependent measurements have been performed at $T = 26$ K, and as a consequence the fine structure splitting remains unresolved due to the significant thermal broadening of the line. Our results demonstrate that relevant QD s-shell properties like the excitonic *fine structure*, the *relative emission strengths* and *spectral widths*, as well as the *power broadening* of these μ -PL lines can be accurately monitored via the almost background-free mode emission.

Moreover, in the following we demonstrate that the QD *emission saturation* and the *photon statistics* under resonant s-shell excitation can also be conveniently measured via the coupled micro-pillar mode. **Figure 4a** depicts results of a power series on a resonantly

(s-shell) pumped single QD for an emitter-mode detuning of $\Delta E = +200 \mu\text{eV}$, monitored via the fundamental cavity mode. We observe the characteristic saturation behavior of a resonantly pumped single quantum dot [20]. The experimental data has been fitted by a theoretical model [21] to describe the emission saturation of a resonantly excited two-level system (see also methods section). Under the given experimental conditions we obtain fit values of $T_1 = 670 \pm 50$ ps for the radiative lifetime and $T_2 = 460 \pm 50$ ps for the emission coherence. With respect to the radiative lifetime of the decay, high conformity is found from a comparison with the results of independent time-resolved spectroscopy measurements (TCSPC; see inset in **Fig. 4a**), yielding a value of $T_1 = 650 \pm 20$ ps.

Figure 4b displays the auto-correlation measurement of another resonantly (s-shell) pumped single QD (pillar 3) with a large emitter-mode detuning of $\Delta E = +440 \mu\text{eV}$. Under purely resonant ($\delta = 0$) pumping of the QD s-shell, the correlation was taken on the coupled fundamental cavity mode signal (see inset spectra). For the regime of low excitation powers applied in the experiment, a single correlation-'dip' but no oscillatory behaviour is expected for the $g^{(2)}(\tau \sim 0)$ trace around zero delay (see methods section). Indeed, very pronounced photon anti-bunching is found in the measured data from the pillar mode with $g^{(2)}(0) \approx 0.26$, derived from a convoluted fit to the experimental trace (bold red line) under consideration of the temporal resolution t_{IRF} of our setup. Applying the same fit parameters (i.e. T_1 and T_2 under the given conditions) as before, but assuming now *full* temporal resolution (as shown by the de-convoluted dashed curve), even the ideal case of $g^{(2)}(0) = 0.0(2)$ for a single quantum emitter is achieved. In clear contrast to the *background-limited* conditions of *p-shell excitation* discussed in **Fig. 1e**, the data of **Fig. 4b** nicely demonstrates the absence of background light, i.e. pure single-photon emission under the given conditions of strictly resonant excitation into the QD s-shell, monitored via a non-resonantly coupled pillar mode.

As a concluding remark, we envision that the demonstrated technique of resonance fluorescence emission 'monitoring' via efficient non-resonant emitter-mode coupling in a micro-resonator represents a very versatile and powerful tool for fundamental studies on the single quantum-dot level. The large coupling efficiencies demonstrate the exciting potential of this technique for resonantly pumped single-photon sources with negligible background. Under proper conditions, even a high degree of photon indistinguishability can be anticipated [9]. In general, the technique should be applicable to a large variety of state-of-the-art micro-cavity geometries, thus allowing for cavity-QED studies with unprecedented detail.

Methods Summary

We use single (In,Ga)As/GaAs quantum dots (QDs) in all-epitaxial high-quality vertical cavity micro-pillar cavities to study in detail the effect of non-resonant emitter-mode coupling at cryogenic temperatures $T < 30$ K. For these investigations a novel sample design and measurement geometry is chosen, providing optical access to individual micro-cavity pillar structures close to a cleaved edge of the sample structure. Optical laser excitation in the lateral plane of QD growth is combined with emission detection along the vertical pillar axis. This technique provides an enhanced separation of resonance fluorescence from scattered laser signal with sufficient signal-to-noise contrast. Resonant s-shell excitation of single QDs is provided by a continuous-wave (cw) narrow-band (500 kHz) tunable Ti:Sapphire laser with 30 GHz scan range. By controlled utilization of the different temperature-dependence of cavity mode spectra and QD s-shell states, a systematic study of the non-resonant emitter-mode coupling effect in 'Stokes' and 'Anti-Stokes' configurations is enabled. The high efficiency of this coupling mechanism is used for a background-free 'monitoring' of numerous essential QD s-shell properties via the coupled (and detuned) pillar mode emission.

Acknowledgements

The authors gratefully acknowledge financial support by the DFG research groups FOR 730 "Positioning of Single Nanostructures – Single Quantum Devices" and FOR 485 "Quantum Optics in Semiconductor Nanostructures". We also thank M. Emmerling and A. Wolf for expert sample preparation.

-
- [1] Michler, P. *et al.* A Quantum Dot Single-Photon Turnstile Device. *Science* **290**, 2282 (2000).
 - [2] Moreau, E. *et al.* Single-mode solid-state single photon source based on isolated quantum dots in microcavities. *Appl. Phys. Lett.* **79**, 2865 (2001).
 - [3] Hennessy, K. *et al.* Quantum nature of a strongly coupled single quantum dot-cavity system. *Nature* **445**, 896 (2007).
 - [4] Press, D. *et al.* Photon antibunching from a single quantum-dot-microcavity system in the strong coupling regime. *Phys. Rev. Lett.* **98**, 117402 (2007).

- [5] Badolato, A., Winger, M., Hennessy, K. J., Hu, E. & Imamoglu, A. Cavity qed effects with single quantum dots. *C. R. Physique* **9**, 850 (2008).
- [6] Kaniber, M. *et al.* Investigation of the nonresonant dot-cavity coupling in two-dimensional photonic crystal nanocavities. *Phys. Rev. B* **77**, 161303(R) (2008).
- [7] Naesby, A., Suhr, T., Kristensen, P. T. & Mørk, J. Influence of pure dephasing on emission spectra from single photon sources. *Phys. Rev. A* **78**, 045802 (2008).
- [8] Yamaguchi, M., Asano, T. & Noda, S. Photon emission by nanocavity-enhanced quantum anti-zeno effect in solid-state cavity quantum-electrodynamics. *Optics Express* **16**, 18067 (2008).
- [9] Auffèves, A., Gérard, J.-M. & Poizat, J.-P. Pure emitter dephasing: a resource for advanced solid-state single photon sources. *arXiv:0808.0820v4 [quant-ph]* (2009).
- [10] Tarel, G. & Savona, V. Emission spectrum of a quantum dot embedded in a nanocavity. *arXiv:0811.0300v1 [cond-mat]* (2008).
- [11] Bouwmeester, D., Ekert, A. & Zeilinger, A. *The Physics of Quantum Information – Quantum Cryptography, Quantum Teleportation, Quantum Computation* (Springer Berlin, 2000).
- [12] Vahala, K. J. Optical microcavities. *Nature* **424**, 839 (2003).
- [13] Santori, C., Fattal, D., Vucković, J., Solomon, G. S. & Yamamoto, Y. Indistinguishable photons from a single-photon device. *Nature* **419**, 594 (2002).
- [14] Reithmaier, J. P. *et al.* Strong coupling in a single quantum dot-semiconductor microcavity system. *Nature* **432**, 197 (2004).
- [15] Yoshie, T. *et al.* Vacuum rabi splitting with a single quantum dot in a photonic crystal nanocavity. *Nature* **432**, 200 (2004).
- [16] Peter, E. *et al.* Exciton-photon strong-coupling regime for a single quantum dot embedded in a microcavity. *Phys. Rev. Lett.* **95**, 067401 (2005).
- [17] Strauf, S. *et al.* Self-tuned quantum dot gain in photonic crystal lasers. *Phys. Rev. Lett.* **96**, 127404 (2006).
- [18] Michler, P. *et al.* Quantum correlation among photons from a single quantum dot at room temperature. *Nature* **406**, 968 (2000).
- [19] Bayer, M. *et al.* Fine structure of neutral and charged excitons in self-assembled in(ga)as/(al)gaas quantum dots. *Phys. Rev. B* **65**, 195315 (2002).
- [20] Stuffer, S., Ester, P., Zrenner, A. & Bichler, M. Power broadening of the exciton linewidth in

- a single ingaas/gaas quantum dot. *Appl. Phys. Lett.* **85**, 4202 (2004).
- [21] Flagg, E. B. *et al.* Resonantly driven coherent oscillations in a solid-state quantum emitter. *Nature Physics*, *adv. online publication* (2009).
- [22] Löffler, A. *et al.* Semiconductor quantum dot microcavity pillars with high-quality factors and enlarged dot dimensions. *Appl. Phys. Lett.* **86**, 111105 (2005).
- [23] Hanbury Brown, R. & Twiss, R. Q. Correlation between photons in two coherent beams of light. *Nature* **177**, 27 (1956).
- [24] Muller, A. *et al.* Resonance fluorescence from a coherently driven semiconductor quantum dot in a cavity. *Phys. Rev. Lett.* **99**, 187402 (2007).
- [25] Brouri, R., Beveratos, A., Poizat, J.-P. & Grangier, P. Photon antibunching in the fluorescence of individual color centers in diamond. *Opt. Lett.* **25**, 1294 (2000).
- [26] Becher, C. *et al.* Nonclassical radiation from a single self-assembled inas quantum dot. *Phys. Rev. B* **63**, 121312(R) (2001).
- [27] Wrigge, G., Gerhardt, I., Hwang, J., Zumofen, G. & Sandoghdar, V. Efficient coupling of photons to a single molecule and the observation of its resonance fluorescence. *Nature* **4**, 60 (2008).

Figure 1: Photon statistics of a non-resonantly coupled QD-micro-pillar cavity system. **a**, Low-temperature ($T = 22$ K) micro-photoluminescence spectra of the s-shell of a single (In,Ga)As/GaAs QD coupled to the spectrally detuned fundamental mode of a micro-pillar cavity (pillar 1). In this case, optical excitation of the QD is applied via laser absorption in the first excited state (p-shell), ~ 22 meV higher in energy (not shown). Please note that in these μ -PL spectra the resolution is limited to ~ 35 μ eV. **b**, Orthogonal geometry of excitation and detection in our μ -PL experiments: Micro-pillars close to a cleaved sample edge are individually addressed by a focused laser within the lateral QD growth plane; μ -PL emission is detected along the vertical micro-pillar axis. **c – e**, Second-order photon auto-correlation measurements on the pure QD or mode emission (traces **c** and **e**, respectively), together with the cross-correlated QD-mode signal (**d**) observed from pillar 1. The bold (dashed) lines represent theoretical fits to the data (open circles), convoluted (de-convoluted) with respect to the detector response time $t_{IRF} = 400$ ps, respectively.

Figure 2: Laser δ -frequency scanning over a single quantum dot s-shell resonance for different dot-cavity detunings ΔE . **a** and **b**, Selected spectra from detailed cw-laser resonance scan series of a coupled QD-cavity system (pillar 2) for the case of *positive* ($\Delta E = +200$ μ eV at $T = 10$ K) and *negative* ($\Delta E = -380$ μ eV at $T = 29$ K) spectral QD-mode detuning. In full consistence with the experimental findings from several studied coupled QD-cavity systems, either case of QD-mode detuning ΔE indicates a strong non-resonant coupling mechanism between the resonantly excited QD fluorescence and the micro-pillar mode emission. As demonstrated in series **a** and **b**, maximum QD resonance fluorescence under s-shell excitation (i.e. laser detuning $\delta = 0$ GHz) consistently appears with maximum 'Stokes' ($\Delta E > 0$) or 'anti-Stokes' ($\Delta E < 0$) mode signal. **c**, Normalized mode emission ratio as a function of QD-mode detuning $\Delta E(T)$, demonstrating increasing mode emission with increasing detuning (i.e. temperature T) from the coupled single QD.

Figure 3: Monitoring single QD s-shell emission properties via a non-resonantly coupled pillar mode. **a, b**, High-resolution s-shell resonance scan (frequency step width: ~ 270 MHz) on the single QD in micro-pillar 2, taken at $T = 18$ K under low excitation power ($P_0 = 100$ nW). Laser tuning over the s-shell clearly reveals a structural asymmetry-induced *fine structure* doublet signature with $\Delta E_{FSS} = 11.3 \pm 0.3 \mu\text{eV}$ in the spectrally integrated emission intensity (trace **b**), which is composed of QD resonance fluorescence and scattered laser signal. From a comparison with the mode signal (detuning $\Delta E = +180 \mu\text{eV}$) in trace **a**, detailed 'mapping' of all spectral features of the non-resonantly coupled QD emission is observed. **c, d**, Excitation power-dependent s-shell resonance scan series of the same QD (pillar 2), demonstrating the effect of *power-broadening* for a resonantly pumped two-level system (trace **d**). A high level of consistence with corresponding data from the coupled mode emission in **c** is found. Note that due to an increased sample temperature of $T = 26$ K, emission fine structures remain unresolved in this case.

Figure 4: QD emission saturation monitoring via a coupled micro-pillar mode. **a**, Power series of the resonantly (s-shell) pumped single QD inside pillar 2 for a QD-mode detuning of $+200 \mu\text{eV}$. Data points represent the spectrally integrated emission signal of the non-resonantly coupled micro-pillar mode. The denoted values of T_1 (radiative lifetime) and T_2 (coherence length) are temperature-sensitive fit parameters to the data. The value of T_1 has been independently verified by time-resolved spectroscopy (TCSPC; see inset figure) under p-shell excitation. **Monitoring of single-photon generation from a resonantly excited QD.** **b**, Photon auto-correlation measurement on the fundamental mode emission of another coupled QD-mode system (pillar 3; $\Delta E = +440 \mu\text{eV}$) under weak ($P_0 = 300$ nW) and purely resonant s-shell excitation of the dot. Despite the large detuning from the emitter, the mode signal fully reflects the *ideal* case of background-free single-photon emission from the coupled QD. The bold (dashed) lines represent theoretical fits to the $g^{(2)}(\tau)$ data, convoluted (de-convoluted) with respect to the temporal setup resolution.

Figure 1

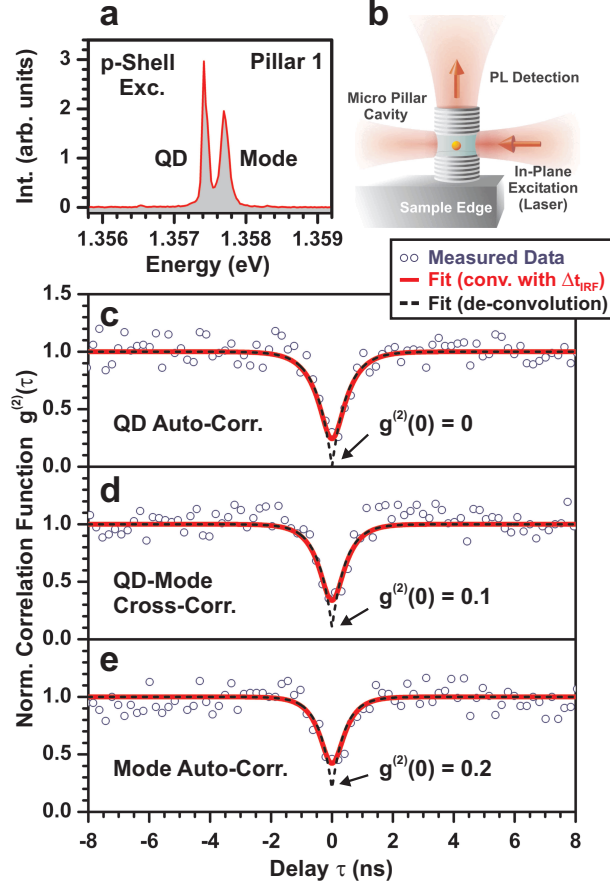


Figure 2

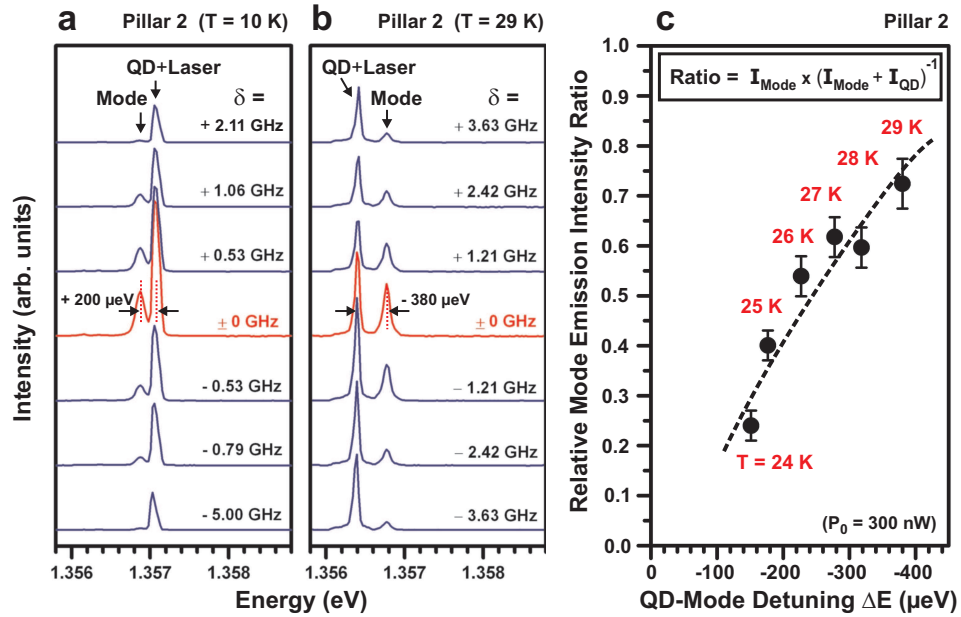


Figure 3

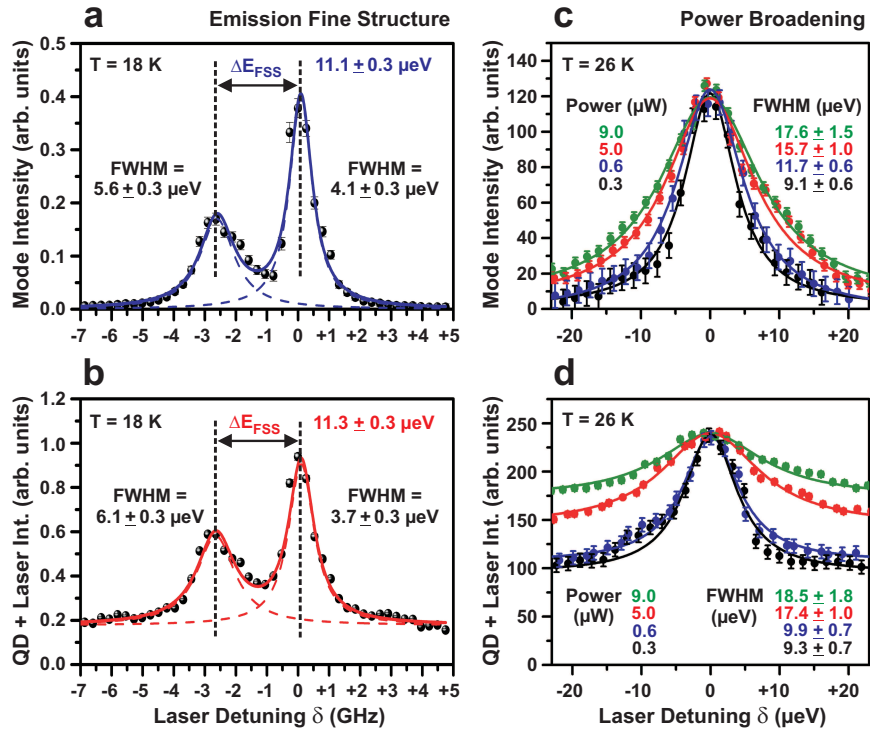
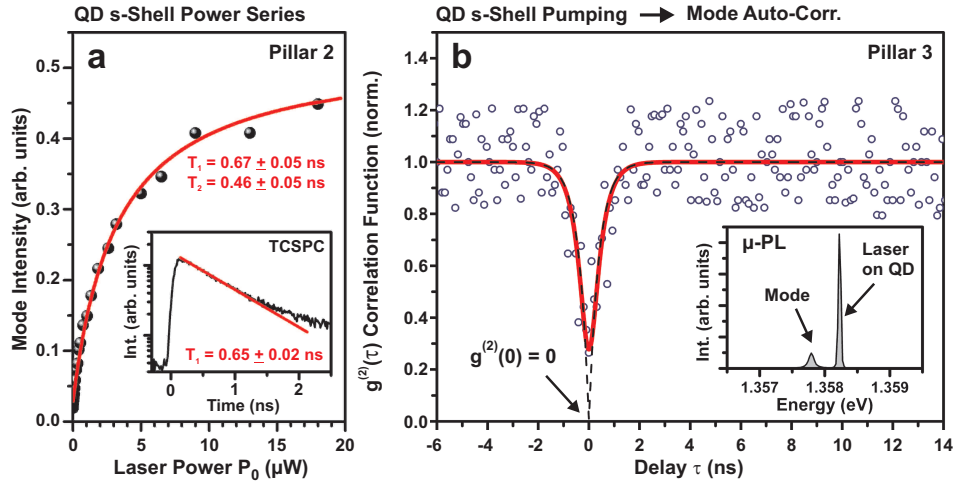


Figure 4



Methods

Sample Growth and Preparation

Our samples were grown by molecular beam epitaxy on a GaAs substrate. The initial planar sample structure consists of a single layer of self-assembled (In,Ga)As QDs (indium content $\sim 45\%$; lateral QD density $\sim 10^{10} \text{ cm}^{-2}$) which is positioned at the center of a 1λ -thick GaAs barrier layer. On top and below the central cavity layer, 26 and 30 periods of alternating $\lambda/4$ -thick layers of AlAs/GaAs were grown to form distributed Bragg reflectors (DBRs), respectively. Micro-pillar resonator arrays were fabricated by a combination of electron-beam lithography and reactive ion etching, details of which are described in [22]. For our studies we have cleaved the structured sample along the major orientation axes of the micro-pillar arrays, leaving a lateral distance of less than $5 \mu\text{m}$ between the outer row of pillars and the sample edge for optimum optical access. A single pillar structure contains only 150-250 QDs on average which are additionally spectrally spread due to their inhomogeneous distribution within the whole dot ensemble (peak position at 1.37 eV ; FWHM $\sim 100 \text{ meV}$).

Experimental Setup

In our studies, the sample was mounted in a cold-finger He-flow cryostat and stabilized to temperatures of $T \leq 30 \text{ K}$ with $\pm 0.5 \text{ K}$ accuracy. Optical excitation of individual micro-pillars was provided by either a tunable narrow-band ($\Delta\nu = 500 \text{ kHz}$ (FWHM)) continuous-wave (cw) Ti:Sapphire ring laser or by a mode-locked tunable Ti:Sapphire pulse laser (76 MHz repetition rate; $\sim 2 \text{ ps}$ pulse width) used in time-resolved micro-photoluminescence (TCSPC). A computer-controlled 3D-precision scanning stage equipped with a 50x microscope (fiber-coupled, SLWD, NA = 0.45) was horizontally adapted to the cryostat unit and used for selective optical excitation of QDs within their lateral growth plane. **Fig. 1b** schematically depicts the orthogonal geometry of excitation and emission detection (50x microscope, SLWD, NA = 0.45) along the vertical micro-pillar axis. This setup allows for a repetitive and long-term stable addressing of individual micro-pillars under strong suppression of scattered laser stray light. Stray light suppression was additionally improved by use of adjustable pin-holes (PH) within the detection path towards the monochromator (not shown), which limit the area of detection in the focal plane to an effective spot diameter

of $\sim 2 \mu\text{m}$. The collected light was spectrally dispersed by one or two 1200 line/mm grating spectrometers each equipped with a ℓN -cooled high-sensitivity charge-coupled device (CCD) camera for time-integrated photon acquisition. To investigate the photon emission statistics, a Hanbury Brown and Twiss-type (HBT) setup [23] for $g^{(2)}(\tau)$ second-order auto-correlation measurements was used. In these correlation measurements, the collected and spectrally pre-filtered photon stream is divided by a 50/50 non-polarizing beam splitter into two symmetric paths, each equipped with an avalanche photo diode (APD) for efficient single-photon detection. Using a time-to-amplitude converter to transform the measured time separations $\tau = t_{\text{stop}} - t_{\text{start}}$ of photon coincidences between the designated 'start' and 'stop' APD channels, the full correlation is stored into a multichannel analyzer. Limited by the response time of the APDs, our HBT setup provides a full temporal resolution of $\Delta t_{\text{res}} \approx 400$ ps. As discussed in the main text, a correct interpretation of the quality of single-photon generation in terms of 'anti-bunching' in $g^{(2)}(\tau)$ measurements demands data de-convolution with the instrumental temporal response function (here: Gaussian profile of FWHM Δt_{IRF}).

Theoretical Data Analysis

According to the theoretical expectations for a *resonantly pumped two-level system* under zero laser detuning $\delta = 0$ [21, 24], the emission rate (i.e. intensity) of spontaneous recombination from the excited state obeys the relation

$$I_{\text{res}}(P_0) \propto \frac{1}{2} \frac{\Omega^2 \cdot T_1/T_2}{T_2^{-2} + \Omega^2 \cdot T_1/T_2} . \quad (1)$$

According to this expression, emission saturation is expected for a regime of strong excitation where $\Omega^2 \gg 1/\sqrt{(T_1 T_2)}$. In order to enable an explicit fit to our experimental example data shown in **Fig. 4a**, the proportionality $\Omega^2 = \beta P_0$ between excitation power P_0 and effective Rabi frequency has been substituted in the above expression. By consideration of the independently verified values of T_1 (radiative life time) and coherence $T_2 = 2\hbar/\Gamma_0$ (with Γ_0 as the zero-power limit of emission linewidth), high conformity is achieved with the experimental mode emission saturation behaviour, which therefore reflects the characteristics of the coupled, resonantly pumped QD. We like to emphasize that the exact value of T_1 strictly depends on the actual Purcell enhancement, i.e. the ΔE detuning-dependent

emitter-mode coupling. In temperature-dependent tuning experiments, the value of T_2 is influenced by the effect of pure dephasing by phonon coupling which increases the emission linewidth with increasing temperature T .

Investigations on the photon emission statistics have been performed under the conditions of either (a) *off-resonant* excitation into the first excited (p-shell) state of single QDs (see **Fig. 1c - e** as well as (b) *purely resonant* excitation into the QD s-shell (**Fig. 4b**). In either case, the raw correlation data is normalized to the expectation value of correlation events for a Poisson-distributed source, i.e. $N_{Poisson}^{cw} = N_{start} \cdot N_{stop} \cdot \Delta t_{int} \cdot \Delta t_{MCA}$ [25]. In this expression, $N_{start,stop}$ correspond to the detector count rates, Δt_{int} represents the total time of integration, and Δt_{MCA} is the temporal bin width of a single channel of the multi-channel analyzer used for accumulation.

(a) As is demonstrated by the dashed lines in **Figs. 1c - e** for the case of *off-resonant excitation*, the Poisson-normalized correlation data traces can be described by a simple theoretical expression [26] of the form

$$g^{(2)}(\tau) = 1 - \rho^2 \exp(-|\tau|/t_m) \quad . \quad (2)$$

In this notation, $\rho = S/(S + B)$ represents the signal-to-background ratio of the detected μ -PL signal, t_m is the (excitation power-dependent) anti-bunching time constant, and $\tau = t_{stop} - t_{start}$ is the measured photon-photon delay, respectively. In order to additionally account for the limited temporal resolution of the detection system, the above expression has to be convoluted by the instrumental response function, which was assumed Gaussian-shaped with $2\sigma \approx \Delta t_{IRF} = 400$ ps in our case. As is discussed in the text, the convoluted function (bold traces) reveals good quantitative agreement with the experimental $g^{(2)}(\tau)$ data, allowing for a correct interpretation of the quality of single-photon generation.

(b) Under the conditions of *strictly resonant QD s-shell excitation* [27] and in the limits of *weak optical pumping*, the Poisson-normalized correlation is theoretically expressed by

$$g_{res}^{(2)}(\tau) = 1 - \left(1 - \frac{T_1}{T_2}\right)^{-1} \cdot \exp\left(-\frac{|\tau|}{T_2}\right) - \left(1 - \frac{T_2}{T_1}\right)^{-1} \cdot \exp\left(-\frac{|\tau|}{T_1}\right) \quad . \quad (3)$$

In this weak power regime, no Rabi oscillations are expected. In the above expression, T_1 and T_2 represent the radiative lifetime and the emission coherence time of the transition, respectively. A corresponding fit (dashed line) has been applied to our experimental data in **Fig. 4b**, which reflects single QD resonance emission coupled to a pillar mode. In order to

analyze the influence of limited time resolution, also here a convolution with the instrumental response Δt_{IRF} (bold line) is applied in comparison with the idealized fit of **Eq. 3**. As is discussed in the main text, we could verify the ideal conditions of background-free single-photon emission from the measured mode signal, which fully reflects the expected emission statistics of the coupled QD.